Rotation, pulsations and outbursts in the Be star upsilo Cygni (HD 202904)

Coralie Neiner, Michèle Floquet, Anne-Marie Hubert, Yves Frémat, R. Hirata, S. Masuda, Douglas R. Gies, C. Buil, Christophe Martayan

A&A 437, 257–272 (2005)
DOI: 10.1051/0004-6361:20041901

Astronomy & Astrophysics

Rotation, pulsations and outbursts in the Be star υ Cygni (HD 202904)⋆

C. Neiner[1,2,⋆⋆], M. Floquet[2], A. M. Hubert[2], Y. Frémat[3], R. Hirata[4], S. Masuda[5], D. Gies[6], C. Buil[7], and C. Martayan[2]

[1] RSSD, Estec, ESA, Keplerlaan 1, 2201 AZ Noordwijk ZH, The Netherlands
e-mail: coralie@ster.kuleuven.ac.be
[2] Observatoire de Paris-Meudon, GEPI, UMR 8111 du CNRS, 92195 Meudon Cedex, France
[3] Observatoire Royal de Belgique, 1180 Brussels, Belgium
[4] Department of Astronomy, Kyoto University, Sakyo-ku, Kyoto 606-8502, Japan
[5] Okayama Astrophysical Observatory, National Astronomical Observatory, Kamogata, Okayama 719-0232, Japan
[6] CHARA, Department of Physics and Astronomy, Georgia State University, Atlanta, GA 30303, USA
[7] CNES, 18 rue Edouard Belin, 31401 Toulouse, France

Received 25 August 2004 / Accepted 20 February 2005

Abstract. υ Cyg is a Be star that shows variations at all timescales. We monitored its spectrum for several years from 1998 to 2004 and, in particular, during a spectroscopic multisite campaign in 2000. In this paper we present and analyse the data. We observed several outbursts including an intense one in 2000. Moreover, we found several periods of short-term variations, including two frequencies at 2.95 and 2.6 c d^{-1}, which are well reproduced by models of non radial pulsations with a retrograde mode with $\ell = 3$ and $m = 3$ and a zonal mode with $\ell = 3$ or 4 and $m = 0$, respectively. The stellar rotation is probably also identified at $f \sim 1.5$ c d^{-1}, which is coherent with the rotation frequency deduced from our determination of stellar parameters. The peak-to-peak amplitude of variations also seems to vary in time, maybe due to a beating effect between close frequencies, but the resolution in time of our data does not allow us to separate such close frequencies. Finally, a longer timescale variation may be present, with a period around 11 years, which could be associated with a binary companion.

Key words. stars: emission-line, Be – stars: activity – stars: individual: υ Cyg – stars: oscillations

1. Introduction

Be stars are non-supergiant B stars that at least once showed emission in at least one of their Balmer lines. They often rotate fast and exhibit light and line-profile variations at different timescales. For a complete review, see Porter & Rivinius (2003).

Be stars also often display either enhancements (outbursts) or fadings of their brightness, depending on whether they are seen rather pole-on or equator-on. The study of Be stars during these phases, simultaneously in spectroscopy and photometry, is very important as it could provide new clues to the Be phenomenon. In particular, one could study the link between mass-loss episodes and the pulsational properties of the star. For the star μ Cen, for example, Rivinius et al. (1998) showed that the beating of stellar pulsations modes with closely spaced periods are related to the outbursts of this star. Outbursts are frequent in galactic and magellanic Be stars, especially in the earlier ones (Hubert et al. 2000; Mennickent et al. 2002). However, simultaneous observations of an outburst in spectroscopy and photometry are fairly rare.

υ Cyg (HD 202904, HR 8146, $V = 4.4$) is a well-known Be star seen under an intermediate angle which shows a strong permanent emission at Hα. This star is also known to undergo outbursts, such as the one observed with the Hipparcos satellite. Therefore this star was chosen as the prime target for a spectroscopic study.

In this paper, thanks to the spectroscopic and photometric data obtained for this star, we investigate the non radial pulsations (NRP) and the ejection of material from the star, focusing on the presence of multiperiodicity and beating effect. The history of the observations of υ Cyg and its long-term variations are presented in Sect. 2. The observations and their reduction are described in Sect. 3 and the spectrum is described in Sect. 4. In Sect. 5 the fundamental stellar parameters are derived. The short-term variability of the line profiles and line parameters are studied in Sect. 6. Photometry obtained with Hipparcos is presented in Sect. 7. A discussion is given in Sect. 8, together

⋆ Based on observations obtained at Haute Provence Observatory and Pic du Midi Observatory (France), Kitt Peak National Observatory (USA), and Okayama Astrophysical Observatory (Japan).

⋆⋆ *Current Affiliation*: Institute for astronomy, KU Leuven, Celestijnenlaan 200B, 3001 Leuven, Belgium.

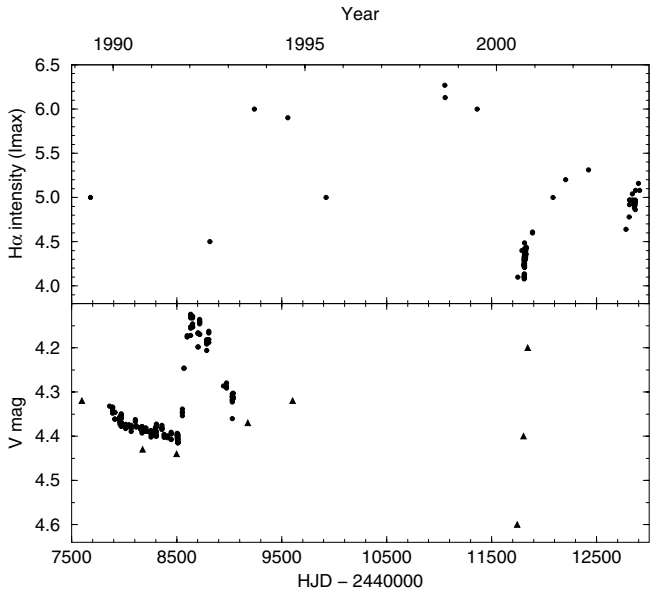

Fig. 1. Long term variability of the Hα line. *Upper panel*: intensity of the line (this paper + Buil 2004); *Lower panel*: Hipparcos photometry (Perryman 1997) and values found in the literature (AAVSO 2003 and Carlsberg Meridian Catalogue 1999).

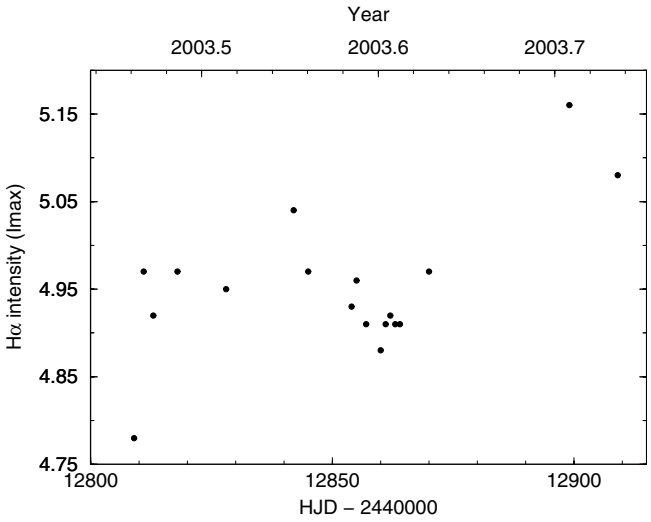

Fig. 2. Maximum intensity of the Hα line observed in 2003 (Buil 2004).

with a model of the stellar atmosphere including pulsations, and is followed by conclusions in Sect. 9.

2. History and long-term variability

υ Cyg has been known as a Be star since the end of the 19th century (Fleming 1891; Campbell 1895). Although the star is bright, it was not regularly observed whether in photometry or in spectroscopy. The Hα line has, however, always been observed in strong emission; according to Peters (1979) the spectrum is stable over several decades. Nevertheless, Hubert-Delplace & Hubert (1979) reported slight variations between 1953 and 1976 with a minimum of emission strength in the first Balmer and Fe II lines from 1969 to 1972.

Spectroscopic data published in the literature since 1976 have confirmed that the Hα emission line is variable: its maximum of intensity ($I_{\rm max}$) ranges from 2.9 in 1983 (Ballereau et al 1987) to 6.3 in 1998 (this paper). The values of $I_{\rm max}$ seem to indicate that additional shorter timescales of about 3–4 years are superimposed on the very long-term variation, which reached a maximum around 1999–2000 (see Fig. 1 and following section).

Photometric data are scarcer than spectroscopic ones, except during the Hipparcos mission (from mid-1989 to mid-1993), which allowed for the first time detection of a strong outburst in this star (Hubert & Floquet 1998; Floquet et al. 2000). This event is characterized by a rapid increase in brightness of 0.3 mag in ~100 days followed by a slow decrease over more than 400 days (see lower part of Fig. 1, HJD 2 447 500-9200). In 2000 (HJD 2 451 750), another strong brightness enhancement of 0.4 mag was observed by amateurs (AAVSO[1]) over ~100 days, simultaneously with our multisite spectroscopic campaign. Such strong outbursts are frequently observed in Be stars seen under a low to moderate angle of inclination either in our Galaxy (Hipparcos observations, Hubert & Floquet 1998; Hubert et al. 2000) or in the Magellanic clouds (OGLE observations, Mennickent et al. 2002).

We note that the temporary decreases in the Hα intensity seem to correspond to episodes of sudden increases in the brightness of the star. This behaviour is observed in several other Be stars, such as 66 Oph (Floquet et al. 2002), HD 58050 (Hubert-Delplace et al. 1982), μ Cen (Rivinius et al. 1998), 28 Cyg (Tubbesing et al. 2000), and HD 76534 (Oudmaijer & Drew 1997). It is often thought that brightness enhancements are associated with mass-loss episodes. In the case of υ Cyg, we deduce from dates of temporary decreases in the Hα intensity (Fig. 1) that the time span between two major outbursts is about 1400 days. Smaller weakening effects in Hα, such as seen in Buil's data (see Fig. 2), could be related to minor outbursts.

3. Observations and data reduction

Several sets of spectroscopic observations were obtained. The log of observations is given in Table 1.

The first set was obtained in 1998 at the Haute Provence Observatory (OHP, France) with the Aurélie spectrograph attached to the 1.52 m telescope. A total of 114 spectra of the He I 6678 line and 2 spectra of the Hα line were obtained with a resolving power of 22 000, a mean exposure time of 40 min and a signal to noise (S/N) ratio of about 600.

The second set of spectroscopic observations was obtained in 2000 at three sites: (i) in France at the Pic du Midi Observatory with the Musicos spectrograph attached to the 2 m Bernard Lyot telescope (TBL) with a resolving power of

[1] We acknowledge with thanks the variable star observations from the AAVSO International Database contributed by observers worldwide and used in this research.

Table 1. Log of spectroscopic observations of υ Cyg.

	Date	HJD - 2 451 000	Line or wav. range (Å)	# sp
	1998/08/28	4.35–4.63	He I 6678	15
			Hα	1
	1998/08/29	5.32–5.64	He I 6678	23
O	1998/08/30	6.35–6.64	He I 6678	23
H			Hα	1
P	1998/08/31	7.32–7.57	He I 6678	14
	1998/09/01	8.32–8.64	He I 6678	18
	1998/09/02	9.31–9.41	He I 6678	5
	11998/09/03	10.32–10.62	He I 6678	16
	2000/09/21	809.58–809.62	B: 3900–5740	3
		809.32–809.51	R: 5150–8890	15
	2000/09/22	810.34–810.45	Blue	6
		810.53–810.60	Red	5
T	2000/09/23	811.34–811.45	Red	7
B	2000/09/24	812.35–812.46	Blue	6
L		812.54–812.59	Red	4
	2000-09-25	813.52–813.58	Blue	4
		813.33–813.43	Red	6
	2000/09/27	815.35–815.41	Blue	4
		815.50–815.59	Red	6
J	2000/09/18	805.97–806.16	4200–4900	9
a	2000/09/19	806.96–807.22		10
p	2000/09/20	807.96–808.22		14
a	2000/09/24	811.92–812.17		13
n	2000/09/25	812.95–813.03		5
	2000/09/30	817.59–817.85	6400–7100	3
K	2000/10/01	818.67–818.88		3
i	2000/10/02	819.61–819.88		3
t	2000/10/03	820.61–820.88		3
t	2000/10/04	821.61–821.88		3
	2000/10/05	822.61–822.88		3
P	2000/10/06	823.60–823.86		3
e	2000/10/07	824.58–824.88		3
a	2000/10/08	825.57		2
k	2000/10/13	830.77–830.87		2
	2000/12/10	888.63–888.64		2
	2003/08/09	1861.52	3850–7100	1
O	2003/08/11	1863.44		2
H	2003/08/13	1865.64		1
P	2003/08/15	1867.50		1
	2003/08/18	1870.39		1
	2003/08/19	1871.46		1

35 000, a mean exposure time of about 20 min, and a S/N ratio between 100 and 400; (ii) in Japan at Okayama Astrophysical Observatory with the Hides échelle spectrograph attached to the 1.88 m telescope with a resolving power of 60 000, a mean exposure time of 15 min, and a S/N ratio between 350 and 450; and (iii) in the USA at Kitt Peak National Observatory with the 0.9 m coudé-fed telescope, a resolving power of 12 500, an exposure time of 1 min, and a mean S/N ratio of 320.

Additional observations were obtained in 2003 in France at the Haute Provence Observatory with the Elodie échelle spectrograph attached to the 1.93 m telescope, with a resolving power of 43 000, an exposure time between 1 and 6 min, and a S/N ratio between 85 and 200.

Data collected by one of us (CB) since 1993 were also investigated to follow variations in the Hα line intensity. The instruments used to obtain these data are spectrographs with a resolution from 7000 to 10 000 mounted on 12.8 to 21.2 cm telescopes (see Buil 2004).

OHP and Okayama observations were reduced with IRAF[2] using standard techniques for CCD data. TBL observations were reduced with ESpRIT (Donati et al. 1997), while KPNO observations were reduced with local facilities. Bias, flat-fields, and wavelength calibration exposures were regularly obtained each night and used to reduce the data. For all the observations, reference regions were carefully selected for satisfactory determination of the pseudo-continuum over about ±50 Å around the lines. All spectra were corrected for heliocentric velocity.

4. The visible and near infrared spectra

A large wavelength range could be observed in 2000 and 2003. The visible and infrared spectrum of υ Cyg is dominated by strong emission lines of hydrogen (Balmer and Paschen series) and other species, such as Fe II and Si II in the visible, and O I and Ca II in the near infrared. The Balmer emission is seen from Hα to at least Hϵ where a faint emission component is detectable, although it is blended with the Ca II–H interstellar line.

The Hα line is in strong permanent emission. Its shape corresponds to the class 1 L of the classification by Hanuschik et al. (1996). This profile can be generated by a Keplerian disk optically thick in the vertical direction and viewed at a moderate angle of inclination (Hummel & Dachs 1992). It could also be a composite profile resulting from material at different radii of the star ejected by successive outbursts.

In the TBL and KP spectra taken in 2000, Hα shows a gradual and weak increase from $I_{\rm max}$ = 4.22 at HJD 2 451 809 to $I_{\rm max}$ = 4.45 at HJD 2 451 830. The only spectrum obtained 2 months later, at Kitt Peak, shows Hα with the same intensity $I_{\rm max} \sim 4.6$ as the Elodie spectra taken in August 2003 (Fig. 4). The Hβ, Hγ, and Hδ lines show a violet (V) and red (R) double peak emission structure, each with 2 components. Their intensity ratio (V/R) fluctuated during the observations. See Sect. 6.3 for the analysis of these emission peaks. As for the Hα profiles, the quadruple structure of Hβ and Hγ emission profiles can be generated by a high density disk or by multiple rings.

The Paschen lines seen in the TBL data from P11 to at least P24, as well as the lines of O I at 7771-75 and 8446 Å, show a double-peaked emission. The Ca II triplet at 8498, 8542, and 8662 Å blended with Paschen lines is also in emission. Lines of Fe II show a double-peaked emission and seem rather stable over the run in 2000 (Δpeaks = 220 km s^{-1}), but Fe II intensities observed in 2003 seem to be slightly higher (by ∼0.01). The red lines of Si II 6347 and 6371 also show a double-peaked emission.

The He I 6678 line was observed in 1998, 2000, and 2003. In 1998 a strong variability was observed in the emission

[2] IRAF is distributed by the National Optical Astronomy Observatories, which is operated by the Association of Universities for Research in Astronomy (AURA), Inc., under cooperative agreement with the National Science Foundation.

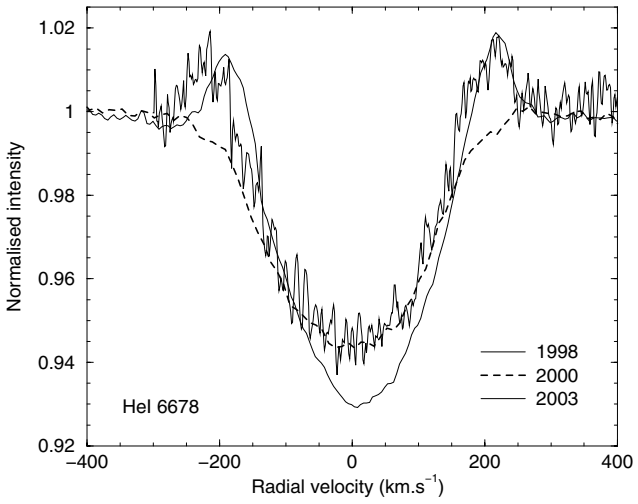

Fig. 3. Mean He I 6678 line profiles observed in 1998, 2000 and 2003.

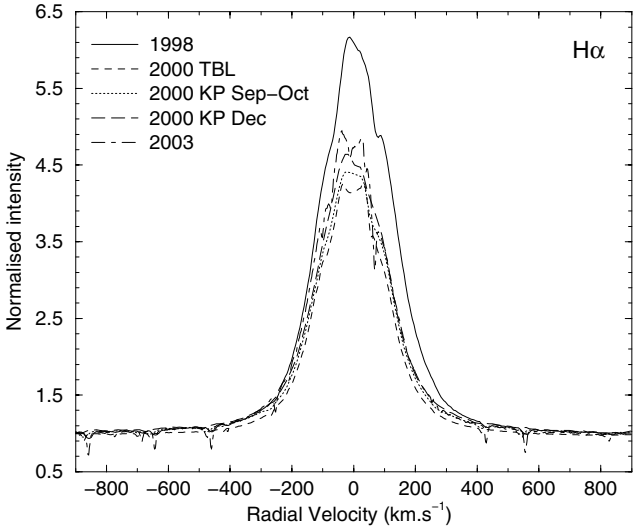

Fig. 4. The Hα line in 1998, 2000, and 2003. In the 2000 data, we separate the mean line profile obtained at TBL, the one obtained at Kitt Peak in September–October, and the only spectrum obtained at Kitt Peak in December.

components, as well as in the absorption part of the line profile (see Fig. 3). In 2000 the profiles of red He I lines (5876, 6678, and 7065) did not show any emission components and the variability was faint. In 2003, when the strength of the Hα line was higher (Fig. 4), the *V* and *R* emission components were again visible in the profile of the He I 6678 line at the end of the run. We note that in 1998, at a time of strong variability, the mean line profile of He I showed a deeper absorption than those in 2000 and 2003, which both have the same depth.

Blue lines of He I, N II, C II, O II, Si II, Si III, and Al III are often polluted by emission lines of Fe II and are thus difficult to study. This is, for example, the case of the Si III triplet at 4553-71 Å.

5. Fundamental parameters

υ Cyg is a fast-rotating Be star. Three main effects are therefore expected to modify the line profiles: (i) emission, mainly present in the hydrogen and Fe II lines; (ii) veiling, due to the continuum light of the circumstellar envelope; and (iii) gravitational darkening, due to fast rotation.

Fundamental parameters of υ Cyg are derived by simultaneously fitting the wings of Hγ and the He I 4388 and 4471 mean line profiles observed in 2000 with modeled spectra produced with the code FASTROT (Frémat et al. 2005). Observations are first corrected for veiling using an empirical procedure described by Ballereau et al. (1995) and measuring the magnitude of the Hγ emission ($W_{H\gamma}$ = 1.3 Å). We find that the veiling correction term r_{4400} we have to account for is equal to 0.30 ± 0.10. This correction strengthens the hydrogen and helium line profiles, as shown in Fig. 5 in which the observations (black dots) are reported both accounting for (case D) and ignoring continuum veiling (case A).

Effects of gravitational darkening due to fast rotation are introduced in the computations using a method similar to the one described by Collins et al. (1991, and references therein). It assumes a Roche model for the stellar deformation and uses von Zeipel's law to compute the temperature for about 10 000 points at the surface of the atmosphere. The local temperature and density distributions are represented by plane parallel model atmospheres computed with ATLAS 9 (Kurucz 1994). We then estimate the NLTE hydrogen and helium level populations with TLUSTY (Hubeny & Lanz 1995) keeping fixed temperature and density distributions. The atomic models we use during these calculations are those available on TLUSTY's webpage, namely H I (9 levels), He I (24 levels), He II (20 levels), and Mg II (25 levels).

For a given fast-rotating star, the computations of the gravitationally darkened synthetic spectra require knowledge of four independent parameters: effective temperature and superficial gravity of the non-rotating stellar counterpart, projected rotation velocity, and relative angular velocity ($\frac{\Omega}{\Omega_c}$ where Ω_c is the break-up angular speed). Masses and radii are directly derived from the Schaller et al. (1992) evolutionary tracks by interpolation on the effective temperature and superficial gravity. The fitting of the hydrogen and helium lines is completed using a least square minimization procedure based on the MINUIT package available at the CERN Program Library.

Effective temperature, superficial gravity, and projected rotation velocity are chosen to be the free parameters of the fit while several values for the angular speed are adopted. According to a statistical study performed by Chauville et al. (2001) and mainly based on the He I 4471 line, Be stars are rotating at 80% of their break-up angular speed. However, following Townsend et al. (2004), gravitational darkening induces saturation of the He I 4471 line width in equator-on fast rotating objects, which would cause underestimation of the mean angular speed of Be stars. Frémat et al. (2005) carried out a careful study of the effects of gravitational darkening on the derived stellar parameters of fast-rotating B-type stars and found that the average rate of angular velocity of Be stars compared to their break-up velocity is 88%. We therefore decided to carry out three different fits of the hydrogen and helium lines, fixing the relative angular speed of the star at 0.80, 0.90, and 0.95.

The results of this procedure are given in Table 2 and labelled C, D, and E. They are compared to Cases A and B

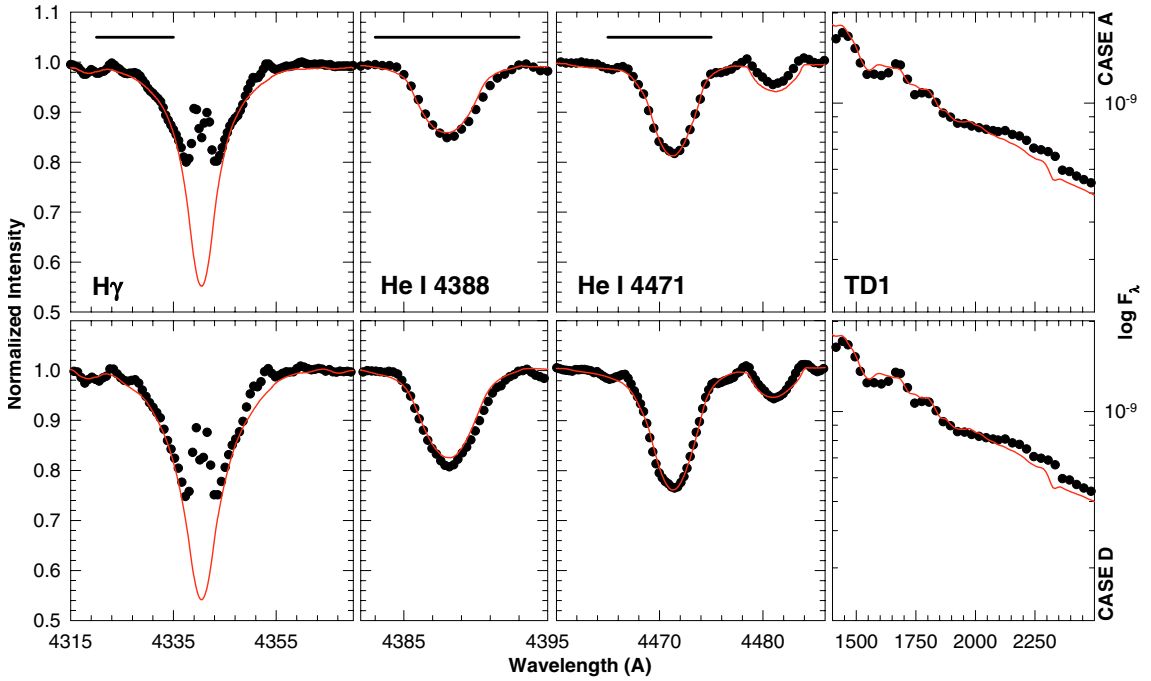

Fig. 5. Line fits (solid line) for Cases A (neither veiling nor gravitational darkening effects) and D (both effects and $\frac{\Omega}{\Omega_c}$ = 90%). The UV TD1 flux is also shown in the right panel. The observations (black dots) are reported accounting for and ignoring continuum veiling in the lower and upper panels respectively.

that are obtained by ignoring veiling effects and gravitational darkening (Case A) and by accounting for the veiling effects but ignoring gravitational darkening (Case B). From Table 2 we note that the strongest effect on the derived fundamental parameters of υ Cyg is related to the continuum veiling whose magnitude varies with time and wavelength. Note also that the temperature, log$g$, and $V \sin i$ increase with $\frac{\Omega}{\Omega_c}$ whereas i decreases.

Figure 5 shows the fits obtained for Cases A and D. When effects of both gravitational darkening and veiling are taken into account, the fits generally show better agreement than for Case A. In all cases, and adopting an $E(B-V)$ of 0.06 derived from the 2200 Å absorption band, our calculations nicely reproduce the UV energy distribution slope observed with the TD1 satellite (right panel in Fig. 5). However, no significant differences are found between the fits carried out for Cases C, D, and E (similar χ^2) and we are thus not able, with this information only, to exclude or select any of the proposed angular velocity values. The only clue might be given by the Hipparcos distance of 276^{+51}_{-37} pc, which seem to indicate a rather high rotation rate ($\frac{\Omega}{\Omega_c} \geq 0.9$) according to the distance determinations of Cases C to E (see Table 2).

Table 2. Stellar parameters obtained from the fits for different cases. Case A is obtained ignoring veiling effects and gravitational darkening; Case B is obtained by accounting only for the veiling effects; for Cases C, D, and E, veiling effects and gravitational darkening are taken into account with a relative angular speed of the star at 80, 90, and 95%, respectively, of its break-up velocity (see Sect. 5).

Case	A	B	
$T_{\rm eff}$ (kK)	17.5 ± 1	19.1 ± 1	
log g (cgs)	3.30 ± 0.10	3.91 ± 0.10	
$v \sin i$ (km s^{-1})	176 ± 5	167 ± 5	
Case	C	D	E
$\frac{\Omega}{\Omega_c}$	0.80	0.90	0.95
$T_{\rm eff}$ (kK)	19.6 ± 1.5	19.8 ± 1.5	20.2 ± 1.5
log g (cgs)	4.04 ± 0.15	4.08 ± 0.15	4.11 ± 0.15
$v \sin i$ (km s^{-1})	170 ± 10	173 ± 10	177 ± 10
$V_{\rm eq}$ (km s^{-1})	312 ± 20	381 ± 25	453 ± 24
i (°)	33 ± 3	27 ± 2	23 ± 2
$T_{\rm pol}$ (kK)	20.6 ± 1.3	21.3 ± 1.4	22.2 ± 1.3
log $g_{\rm pol}$ (cgs)	4.08 ± 0.12	4.13 ± 0.12	4.17 ± 0.12
$R_{\rm pol}$ ($R_\odot$)	3.93 ± 0.70	3.67 ± 0.66	3.55 ± 0.64
$R_{\rm eq}$ ($R_\odot$)	4.62 ± 0.83	4.68 ± 0.83	4.80 ± 0.87
M ($M_\odot$)	6.81 ± 0.81	6.81 ± 0.80	6.97 ± 0.85
L ($L_\odot$)	3.35 ± 0.21	3.32 ± 0.21	3.34 ± 0.22
$f_{\rm rot}$ (c d^{-1})	1.35 ± 0.35	1.63 ± 0.40	1.88 ± 0.46
dist (pc)	205 ± 70	228 ± 80	248 ± 85

6. Short-term variability

A search for short-term variability in line profiles and spectral parameters is performed for the 1998 and 2000 data. The number of spectra obtained in 2003 is insufficient for that purpose. The He I 6678 line is the only photospheric line monitored both in 1998 and 2000. All the other studied lines, i.e. the strong blue photospheric lines He I 4388, 4471 and 4713, C II 4267 and Mg II 4481, as well as the Hβ and Hγ lines affected by emission, were only obtained in 2000. All these lines were intensively observed at two sites (Okayama, Japan and Pic du Midi, France) but unfortunately, due to allocated observing time and bad weather conditions, there is no overlap between these datasets. The number of spectra of the red He I 5876 line is not sufficient to reliably determine frequencies.

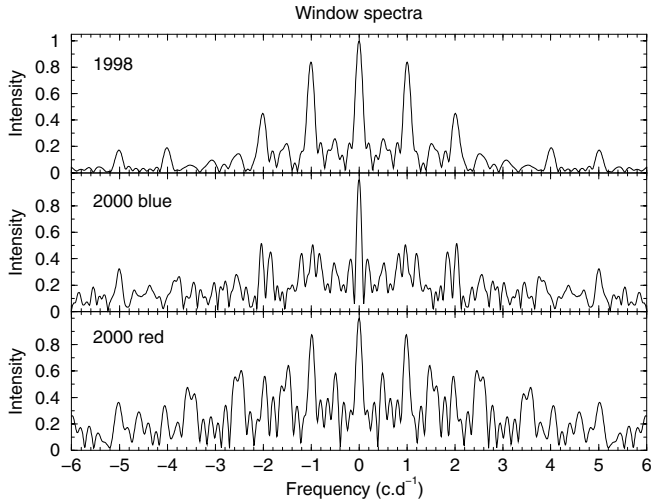

Fig. 6. Window spectra of the observations obtained in 1998 (*upper panel*) and in 2000 (blue spectrum in *middle panel* and red spectrum in *lower panel*).

Moreover, the He I 4921 line is strongly polluted by the Fe II 4923 emission line and therefore not investigated. The Mg II 4481 line is also perturbed on its red wing by Fe II emission lines and the results obtained for this line should thus be considered with caution.

We searched for short-term periodicity in spectral parameters: radial velocity (*RV*) of the line centroid, equivalent width (EW), central depth (CD), $V \sin i$, intensity of V and R emission components when present, as well as their V/R ratio and radial velocity. The first minimum of the Fourier transform of each He I, C II, and Mg II studied line is used to estimate apparent variations in the projected equatorial rotational velocity $V \sin i$ (Gray 1976). Using this method, the estimate of $V \sin i$ is not significantly affected by emission in the line wings (Jankov et al. 2000). For Balmer lines the radial velocity of the whole emission measured at half-maximum intensity is also investigated.

TSA is performed as in Floquet et al. (2000, 2002) by using Fourier Tranform + Clean algorithm and least squares fitting methods. These algorithms are applied to each time series, and the frequency analysis is performed on each resolution bin of line-profile time series. Results are given in Tables 3 and 5. The accuracy of the frequency determination is 0.16 and 0.11 c d^{-1} for the 1998 and 2000 datasets, respectively. The window function for the He I 6678 line in 1998 and 2000, as well as for blue lines having different temporal coverage during the multisite campaign of 2000, is given in Fig. 6.

6.1. He I 6678

The data obtained in 1998 and 2000 are analysed separately because the mean line profiles of the He I 6678 line are different as can be seen in Fig. 3. The 1998 line profiles show a broad absorption component with an average central intensity $I_{\rm min}$ = 0.93 and outer V and R emission peaks (Δ Peaks $\sim$ 400 km s^{-1}). These components are highly variable on a short timescale. In the 2000 data no outer V and R emission components disturb the photospheric line profile, but the average central intensity is higher $I_{\rm min}$ = 0.945 and line-profile variations (*lpv*) are weak. Unfortunately this line is not included in Hides spectra, which have the best S/N ratio of the multisite campaign. Moreover, variability is found to be more conspicuous at the beginning of the run in blue helium lines (see Sect. 6.2), but could only be investigated in detail in the He I 6678 line in the second part of the run with TBL data.

Table 3. Results of the Time Series Analysis for the He I, C II, and Mg II lines obtained with the least squares method. The minimum detectable frequency is 0.16 and 0.11 c d^{-1} in 1998 and 2000, respectively.

Line	Year	*lpv*	*RV*	CD	$V \sin i$
He I 6678	1998	1.50	1.50	2.60	3.02
		3.01		3.04	2.59
		2.64			
		5.98			
He I 6678	2000	1.60		1.63	
He I 4713	2000	1.58	1.57	2.58	2.95
		2.58	2.94		3.61
		3.96			
He I 4471	2000	1.53	1.60	2.57	
		1.60		2.97	
		2.95			
He I 4388	2000	1.60	1.62	2.96	
		2.96	0.58	2.57	
			1.55		
C II 4267	2000	2.57	1.59	2.59	2.95
		2.95	1.68	2.88	3.58
		5.87			
Mg II 4481	2000	1.58		2.57	
		2.58			
		2.94			

6.1.1. Data obtained in 1998

In 1998 *lpv* and all measured quantities (*RV* of the centroid, V and R emission peaks, their sum $V + R$, and the V/R ratio) displayed conspicuous variations (see Fig. 7), which seem to be multiperiodic with V and R varying in opposition of phase. The variance shows maximum amplitude at velocities corresponding to the V and R emission peaks and extends to $\pm$260 km s^{-1}, i.e. outside the boundary $\pm$ $V \sin i$ (see Fig. 8). In *lpv* and in the majority of the measured spectral quantities (*RV* of the centroid, V and R emission peaks, V/R ratio) the main frequency is 1.50 c d^{-1}, but two other ones at 2.6 and 3.0 c d^{-1} are also present, mainly in the CD and $V \sin i$ variations.

The signal power is distributed in a different way across the line profile depending on the frequency (see upper panels of Figs. 9 and 10). The frequency at 1.5 c d^{-1}, which dominates in *lpv*, has a signal power distribution similar to the variance, i.e. very strong in the V and R emission components (see Fig. 8), but its velocity phase is badly defined. Conversely, the frequency at 2.6 c d^{-1} does not have a strong signal power distribution in the V and R emission components, but its velocity phase is also not well defined in the central part of the line with a strong power (upper panel of Fig. 9). The frequency

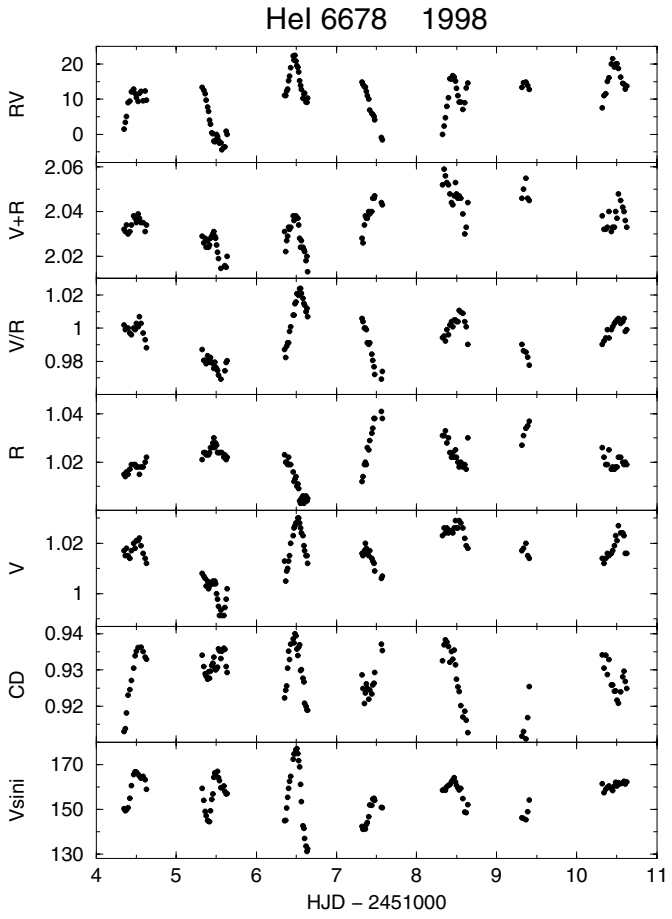

Fig. 7. Variations in time of RV (in km s^{-1}), CD, V, R, V/R, $V + R$ (in normalised intensity), and $V \sin i$ (in km s^{-1}) for the He I 6678 line in 1998.

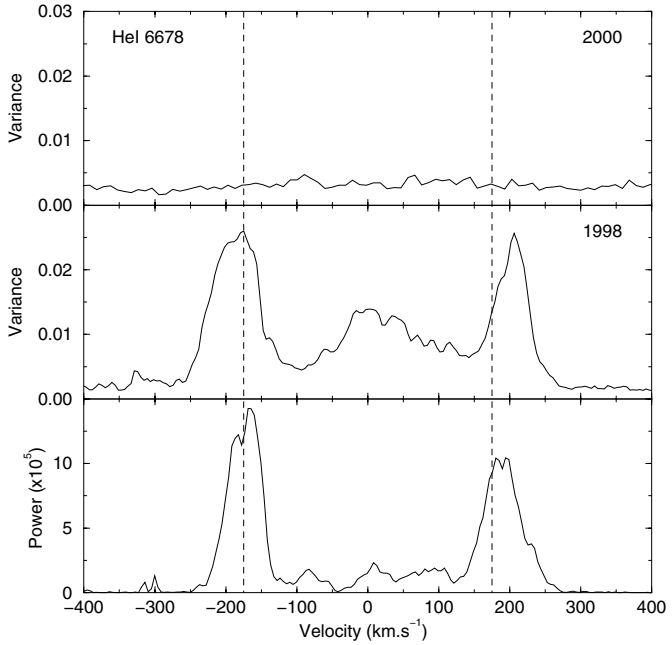

Fig. 8. Variance of the He I 6678 line in 2000 (*upper panel*) and in 1998 (*middle panel*) and power distribution (*lower panel*) of the predominent frequency found in the line at the same epoch $f = 1.50$ c d^{-1}. Dashed lines indicate $\pm V \sin i$.

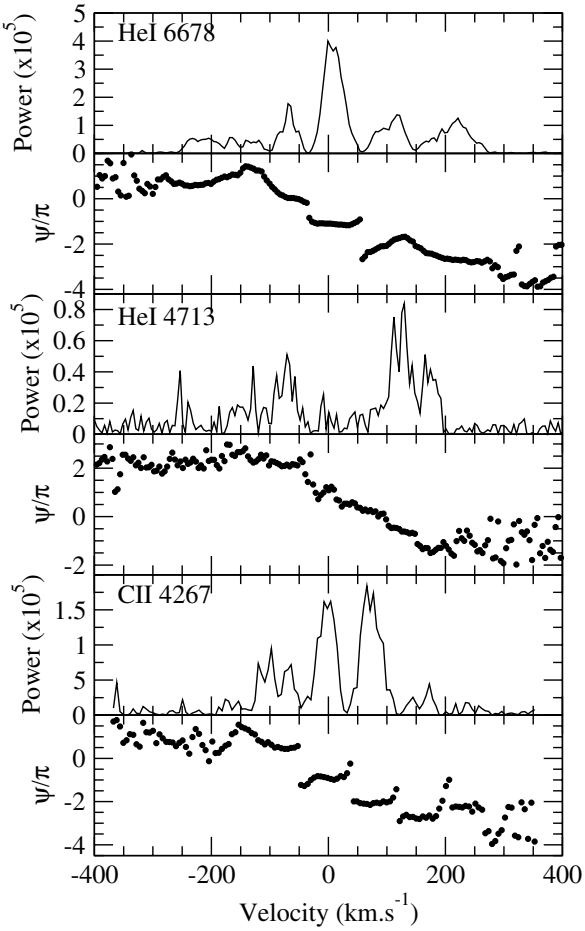

Fig. 9. Phase and power distribution of the frequency $f = 2.6$ c d^{-1} for the He I 6678 line observed in 1998 (*upper panel*), the He I 4713 line (*middle panel*) and the C II 4267 line (*lower panel*).

at 3.0 c d^{-1} is the only one with a coherent velocity phase across the line profile (upper panel of Fig. 10). Its first harmonic appears in the He I 6678 and C II 4267 lines. Estimates of ℓ and m from the slope of the velocity phase are given in Table 4.

Residuals of line profiles, i.e. line profiles from which the mean profile of the 1998 data has been subtracted, are carefully investigated. Greyscale dynamic spectra of the He I 6678 line folded in phase with 2.6 and 3.0 c d^{-1} are shown in Fig. 11. We note that the pattern of dynamical spectra folded with the 2.6 c d^{-1} is quite different from the one folded with 3.0 c d^{-1}.

As found in *lpv*, the frequency at 1.5 c d^{-1} is often dominating in spectral parameter variations, such as in the RV of the absorption centroid and the V/R ratio of emission peaks shown in Fig. 12. However, the maximum and minimum values are different from one night to another. Therefore these variations cannot be fitted with this periodic signal alone. We find that the behaviour of the most conspicuous variations (in CD for instance) can be successfully reproduced with the two frequencies at 2.6 and 2.95 c d^{-1}, except the second day, as shown in Fig. 13. This anomaly on the second day is probably related to a small outburst. Indeed, a rise of the emission level starts on the second day of observations (see $V + R$ in Fig. 7) and lasts until the fifth day.

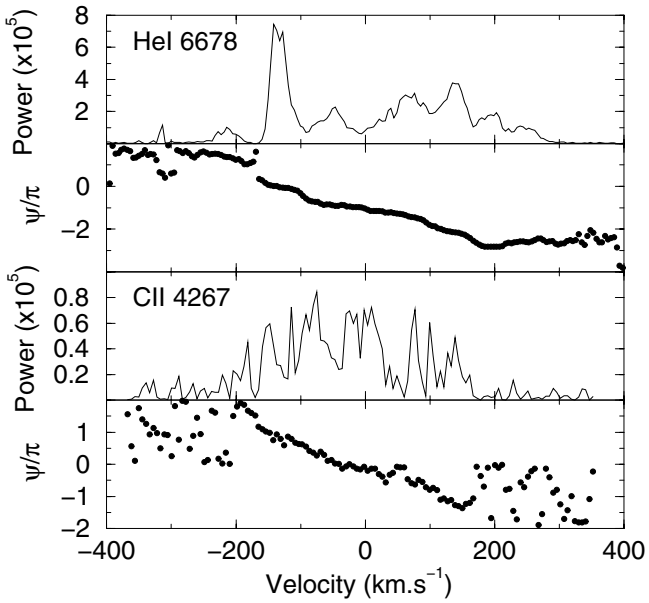

Fig. 10. Phase and power distribution of the frequency $f = 3.0$ c d^{-1} for the He I 6678 line observed in 1998 (*upper panel*) and the C II 4267 line observed in 2000 (*lower panel*).

Table 4. ℓ and m values deduced from the phase difference $\Delta\Psi/\pi$ measured from the phase distribution of different frequencies in the *lpv* of several photospheric lines (see e.g. Figs. 9 and 10).

Line	Year	Freq (c d^{-1})	$\Delta\Psi/\pi$	ℓ	$\|m\|$
He I 6678	1998	1.50	1.9		
		2.64	3.9	4	
		3.01	3.5	3	
		5.98	6.3		3
He I 6678	2000	1.60	–		
He I 4713	2000	1.57	2		
		2.57	3.7	4	
		2.93	2.6	3	
He I 4471	2000	1.60	1.8		
		1.53	–		
		2.95	3.0	3	
He I 4388	2000	1.60	–		
		2.52	2.7	3	
		2.96	3.0	3	
C II 4267	2000	2.57	4.3	4	
		2.95	3.2	3	
		5.87	6.1		3
Mg II 4481	2000	1.58	–		
		2.58	4.7	5	
		2.94	4	4	

Finally, we note a small increase in the $V + R$ quantity between the 6th and the 8th days of the run, similar to the ones observed in EW Lac (Floquet et al. 2000) and ω Ori (Neiner et al. 2002) and typically representative of the short-lived, numerous, faint outbursts reported for early Be stars.

6.1.2. Data obtained in 2000

In the 2000 data, the variance across the line is very small and concentrated within $\pm$ $V \sin i$ (Fig. 8, upper panel). A

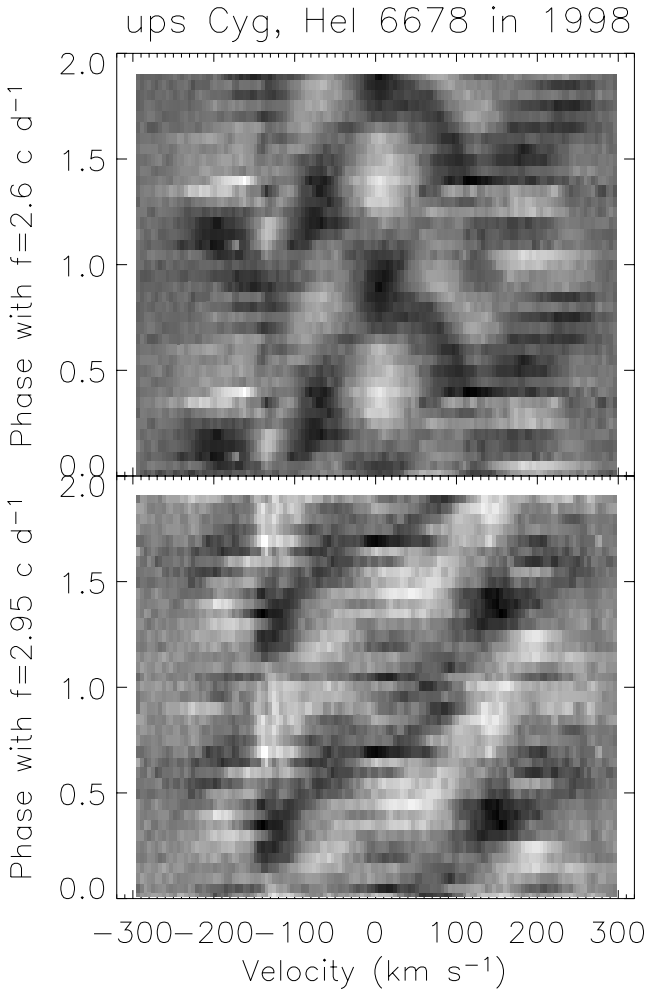

Fig. 11. Greyscale dynamic spectra of the residuals of the He I 6678 line observed in 1998. *Top panel*: folded in phase with $f = 2.6$ c d^{-1}. *Bottom panel*: folded in phase with $f = 2.95$ c d^{-1}.

frequency at 1.6 c d^{-1} is detected in *lpv* and CD. Due to the weakness of the signal and limited accuracy on the frequency determination, we could not discriminate between 1.5 c d^{-1} detected in 1998 and 1.6 c d^{-1} detected in 2000. The latter is probably a 1-day alias of the 2.6 c d^{-1} frequency. Both frequencies are found in the 1998 data.

6.2. Blue photospheric lines

As mentioned above, blue photospheric lines were only monitored during the multisite campaign of 2000. Our study was carried out on the strong helium lines not polluted by Fe II emission (He I 4388, 4471 and 4713), the C II 4267 line, and the Mg II 4481 line. Mean profiles of the He I 4388, 4471, and 4713 lines are presented in Fig. 14. The He I 4471 line seems to be shifted towards blue, which is probably due to the presence of the He I 4469.9 forbidden line and of O II lines on the blue wing of the He I 4471 line. In 2000 the variability observed in these lines was greater than that of red lines, such as the He I 6678 line, but their temporal coverage was different.

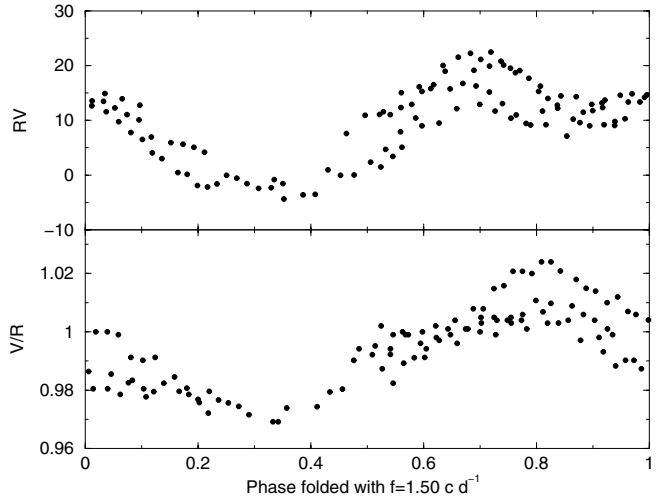

Fig. 12. Radial velocity (in km s^{-1}) of the centroid and V/R ratio of the He I 6678 line observed in 1998, folded in phase with f=1.50 c d^{-1}.

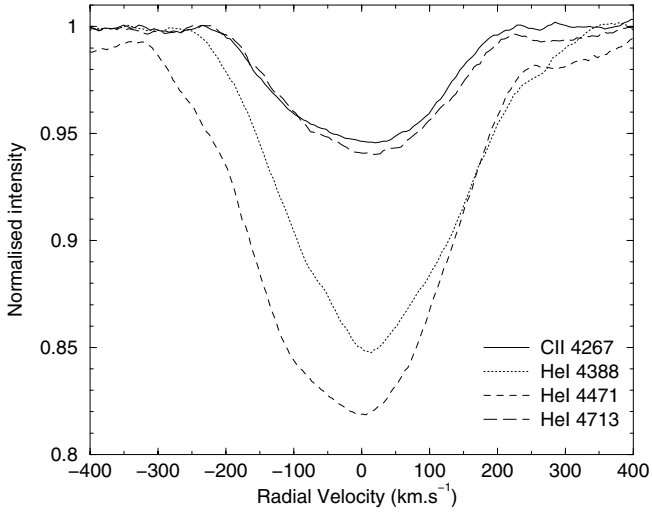

Fig. 14. Mean profiles of the C II 4267 and He I 4388, 4471, and 4713 lines observed in 2000.

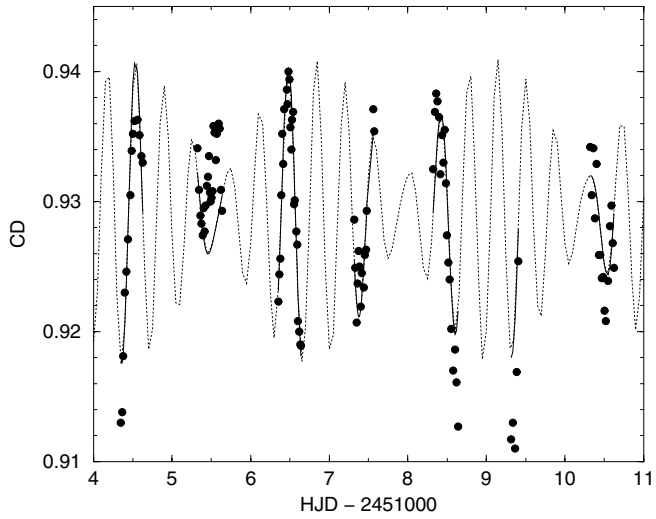

Fig. 13. Variations of CD (in normalised intensity) of the He I 6678 line observed in 1998, together with a sinusoidal fit using the two frequencies at 2.6 and 2.95 c d^{-1}.

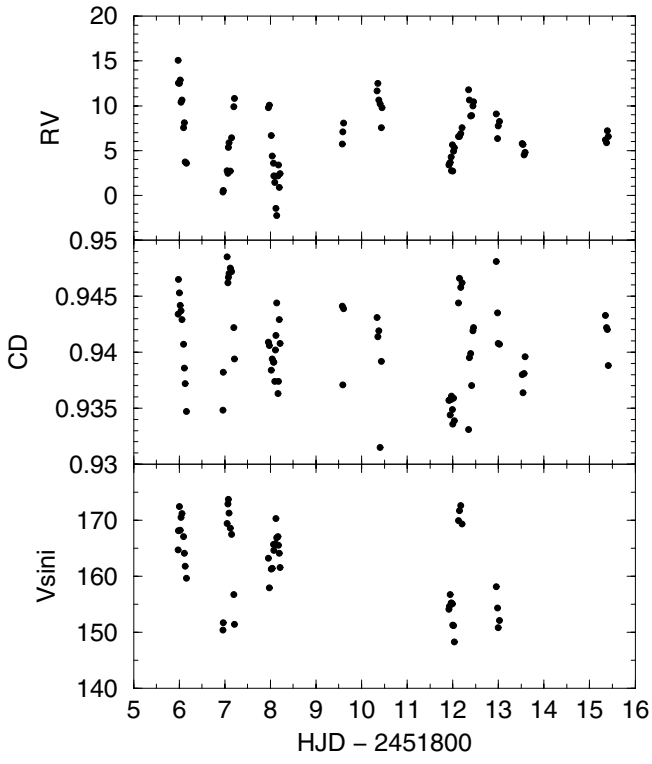

Fig. 15. Variations of RV (in km s^{-1}), CD (in normalised intensity), and $V \sin i$ (in km s^{-1}) for the He I 4713 line in 2000.

Examples of variations of the line parameters RV, CD, and $V \sin i$, when measurable for the latter, are given for the He I 4713 and C II 4267 lines in Figs. 15 and 16, respectively. The total amplitude of the centroid RV variation is more conspicuous at the beginning of the run (about 12.5 km s^{-1}). Afterwards, between the 9th and 13th days, it seems to be only 5 km s^{-1}. This behaviour is very typical of a beating effect.

Results of TSA of *lpv* and of the spectral parameters RV, CD, $V \sin i$ for the blue helium, C II 4267, and Mg II 4481 lines are reported in Table 3. The main frequencies found in the data are at 1.6, 2.6, and 2.95 c d^{-1}. The 2.95 c d^{-1} frequency can be identified with the 3.0 c d^{-1} frequency obtained with the 1998 data within the accuracy of the determination. Figure 10 (bottom panel) shows the power and phase distributions for the C II 4267 line. The first harmonic of the 2.95 c d^{-1} frequency seems to be present in the TSA of the C II 4267 line for which the best spectra were obtained during the campaign of 2000. An example of the power and phase distributions for the 2.6 c d^{-1} frequency across the He I 4713 and C II 4267 lines is given in Fig. 9 (middle and lower panels). Note that for the He I 4713 line, the phase distribution is coherent to the contrary to the He I 6678 line observed in 1998 and to the C II 4267 line. The He I 4713 line also shows no strong power in the centre of the line. The 1.6 c d^{-1} frequency does not have a coherent velocity phase for the He I lines, thus it is interpreted as a 1-day alias of the 2.6 c d^{-1} frequency. In terms of non-radial pulsations, estimates of ℓ and m can be given from the slope of the velocity phase (Telting & Schrijvers 1997) and are reported in Table 4.

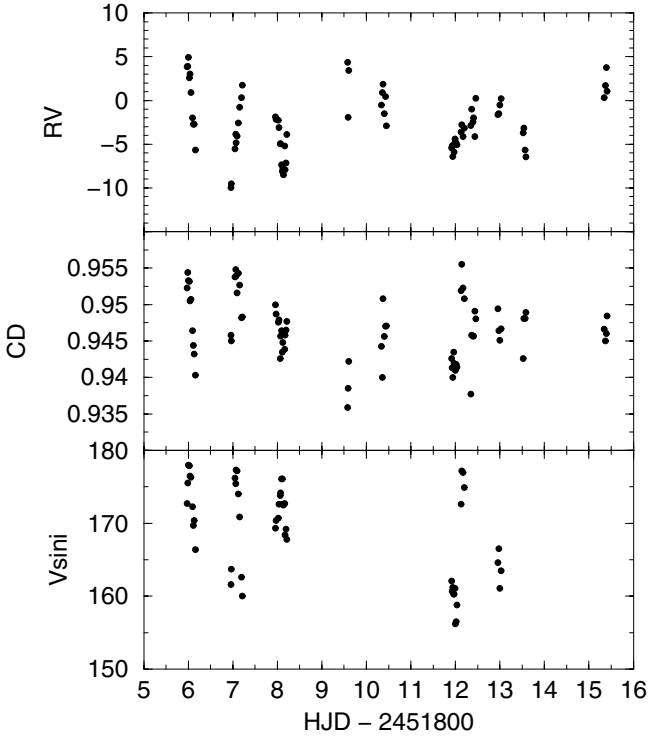

Fig. 16. Variations of RV (in km s^{-1}), CD (in normalised intensity), and $V \sin i$ (in km s^{-1}) for the C II 4267 line in 2000.

Greyscale dynamic residual spectra (i.e. line profiles from which the mean profile of the data from 2000 has been subtracted) of the He I 4713 and C II 4267 lines are shown in Figs. 17 and 18, respectively. Clear patterns appear in these figures.

6.3. Balmer lines

The Hβ and Hγ photospheric lines are affected by a composite circumstellar emission showing two V and R peaks with a double component each, i.e. four emission peaks in total. Each mean line profile and its respective variance are shown in Fig. 19. The peak separation of the inner and outer emission components of the Hβ line leads to a radius of 13.6 and 4.1 R_* respectively, if the material is in two Keplerian orbits (Hummel & Vrancken 1995) and using the stellar parameters determined in Sect. 5. For the Hα line, such profiles can also be explained by a Keplerian disk optically thick in the vertical direction and viewed at a moderate angle of inclination (Hummel & Dachs 1992). Their calculations are made for Balmer lines in general (see Hummel & Dachs 1992) and, thus, could also apply to Hβ and Hγ.

Note that the peak separation of the Fe II lines corresponds to that of the outer emission components (~220 km s^{-1}) of the Hβ and Hγ lines and thus to the material closest to the star, i.e. ejected last. In the data obtained in 2003, however, the peak separation of these Fe II lines corresponds to only 160 km s^{-1}, which means that the material has been moving outwards in the elapsed time.

A search for periodicities is performed in lpv, in the RV of the whole emission measured at half-maximum and in the

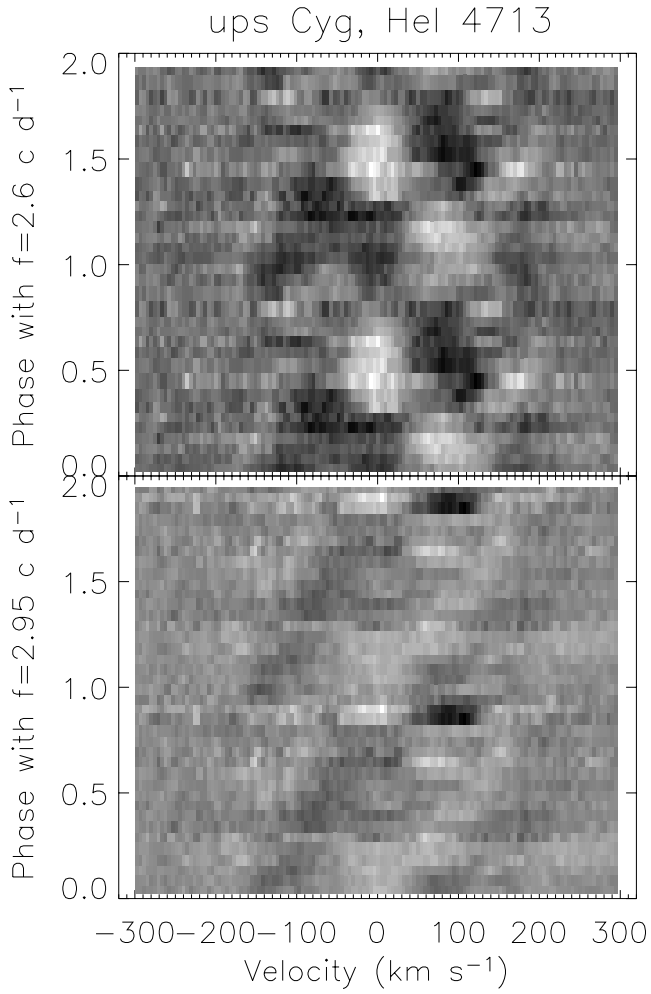

Fig. 17. Greyscale dynamic spectra of the residuals of the He I 4713 line observed in 2000. *Top panel*: folded in phase with f = 2.6 c d^{-1}. *Bottom panel*: folded in phase with f = 2.95 c d^{-1}.

Table 5. Results of time series analysis for the Balmer Hβ and Hγ lines obtained with the least squares method.

Line	year	lpv	RVem	$V1$	$R1$	$V1/R1$	$V2$	$R2$	$V2/R2$
Hβ	2000	0.11	1.55	1.58	3.60	2.54	1.05	2.52	2.61
		1.55	1.45	1.43	0.51		0.57		1.55
		1.46							
		1.64							
Hγ	2000	1.57	1.56	2.57	1.58	1.56	2.58	1.57	1.58
		1.02	1.67	2.77		1.66		2.54	1.65
		2.53	1.43						

double structure of each emission peak of the Hβ and Hγ lines. The dominant frequency is 2.6 or 1.6 c d^{-1} (see Table 5), in agreement with the 2.6 c d^{-1} frequency found in photospheric lines, but no coherent phase distribution is retrieved across the line profiles.

7. Light variability: Hipparcos photometry

Hipparcos observed υ Cyg over a period of 1178 days from mid-1989 to mid-1993, and observed one outburst (see Fig. 1). Several continuous data series were obtained over about one

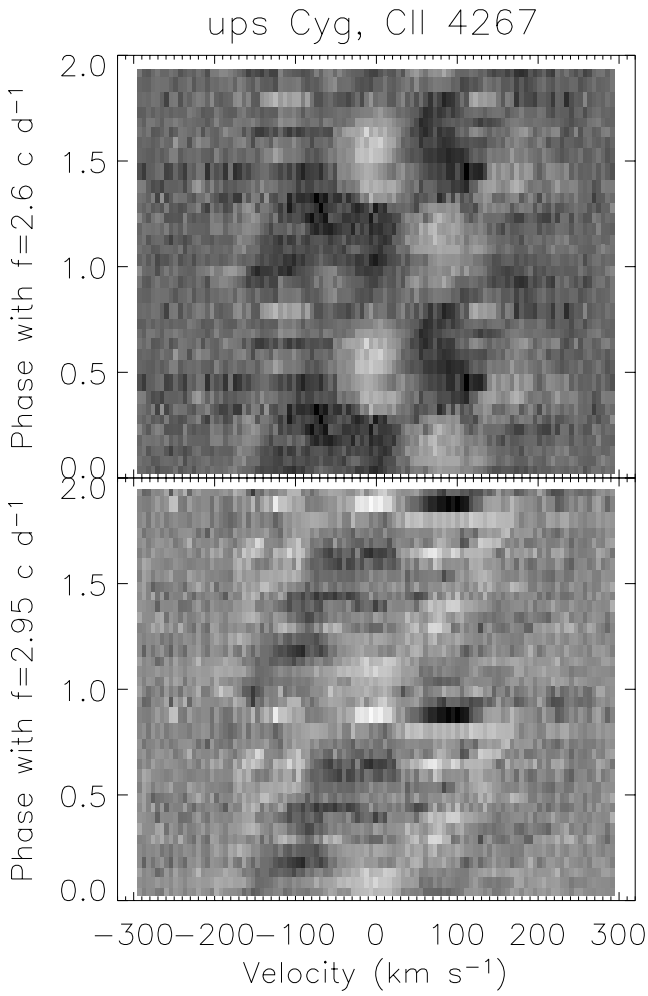

Fig. 18. Greyscale dynamic spectra of the residuals of the C II 4267 line observed in 2000. *Top panel*: folded in phase with $f = 2.6$ c d^{-1}. *Bottom panel*: folded in phase with $f = 2.95$ c d^{-1}.

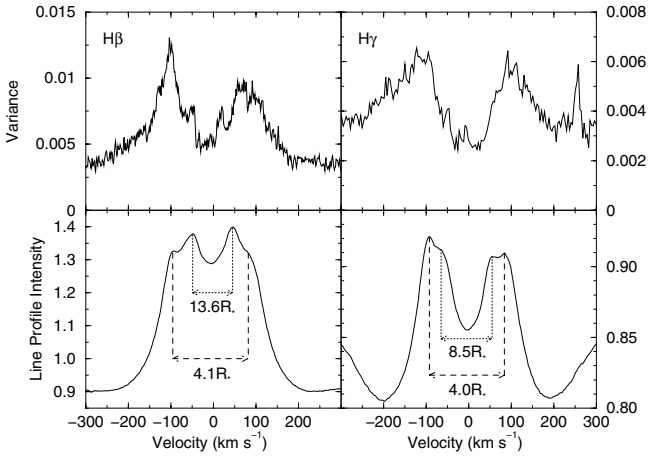

Fig. 19. Line profile and variance of the Hβ (*left*) and Hγ (*right*) observed in 2000.

day each, which also showed short-term variations with a small variable amplitude. Hubert & Floquet (1998) found a frequency of 0.88 c d^{-1} in these data, while Percy et al. (2003) suggest that this corresponds to a double-wave light curve and that the frequency is 0.44 c d^{-1}. The peak-to-peak amplitude of the variations is about 0.02 mag.

8. Discussion

8.1. Outbursts

υ Cyg is a very active Be star that undergoes numerous outbursts. Observations of the He I 6678 line in 1998 were obtained between two major outbursts. According to the weak increase in the $V + R$ quantity (Fig. 7) and to the change of CD variation on the second day of observations (Fig. 13), it seems that a small outburst occured during this observing run. Unfortunately, no photometric data are available from that time.

On the other hand, the multi-site campaign of 2000 took place during a very strong light outburst characterised by a 0.4 mag increase in brightness (see Fig. 1). As for 66 Oph (Floquet et al. 2003), the Hα intensity seems to be anti-correlated with the visual brightness. No conspicuous variation was observed for the He I 6678 line in 2000 (top panel of Fig. 8). The poor variation could be due to the outburst. The He I 5876 and 6678 lines belong to the singlet/triplet 2P – nD series. They are the strongest non resonance He I transitions and thus respond to thermal changes in the superficial atmosphere ($\tau \sim 10^{-3}$) of early B stars (Smith et al. 1994). The outburst of υ Cyg could thus strongly affect these two lines. Moreover, a quadruple emission profile was observed in the Hβ and Hγ lines in 2000 (Fig. 19), which could indicate a Keplerian disk, optically thick in the vertical direction. In that case, following the equations of Hummel & Vrancken (1995), the Hβ emitting material would be at 6.8 R_* and the Hγ emitting material at 5.6 R_*. Such a quadruple profile could also indicate two zones of emitting material at 4.1 and 13.6 R_* for Hβ, and 4.0 and 8.5 R_* for Hγ, probably resulting from two outbursts. The latter explanation is supported by the fact that the peak separation of the Fe II lines decreased from 220 to 160 km s^{-1} from 2000 to 2003, showing that the material is moving outwards with time, with a velocity of about 75 m s^{-1}.

In 2003, we observed a temporary weakening of the emission intensity at Hα and in the He I 6678 line. This can be explained by a veiling effect during an outburst. Figure 20 shows the time variation of the He I 6678 line profile (dots) compared to the theoretical photospheric line. The veiling correction (r_{6678}) needed to directly compare the observations (dashes) to the synthetic spectrum (solid line) is expected to be related to the combination of continuum and line emission due to the ejection and motion of circumstellar material. Line emission was clearly seen in 1998 when the intensity of the Hα line was highest. It was also seen in 2003 when it was decreasing. From additional data obtained in 2003 (Fig. 2), it indeed seems that the OHP data were obtained after a major outburst followed by a smaller outburst. Within 10 days the emission feature reappeared on the blue and red wings of the He I 5876 and 6678 lines. In both cases (1998 and 2003), the emission broke the line profile symmetry, which was not observed in 2000, although the Hα line was as strong as in 2003.

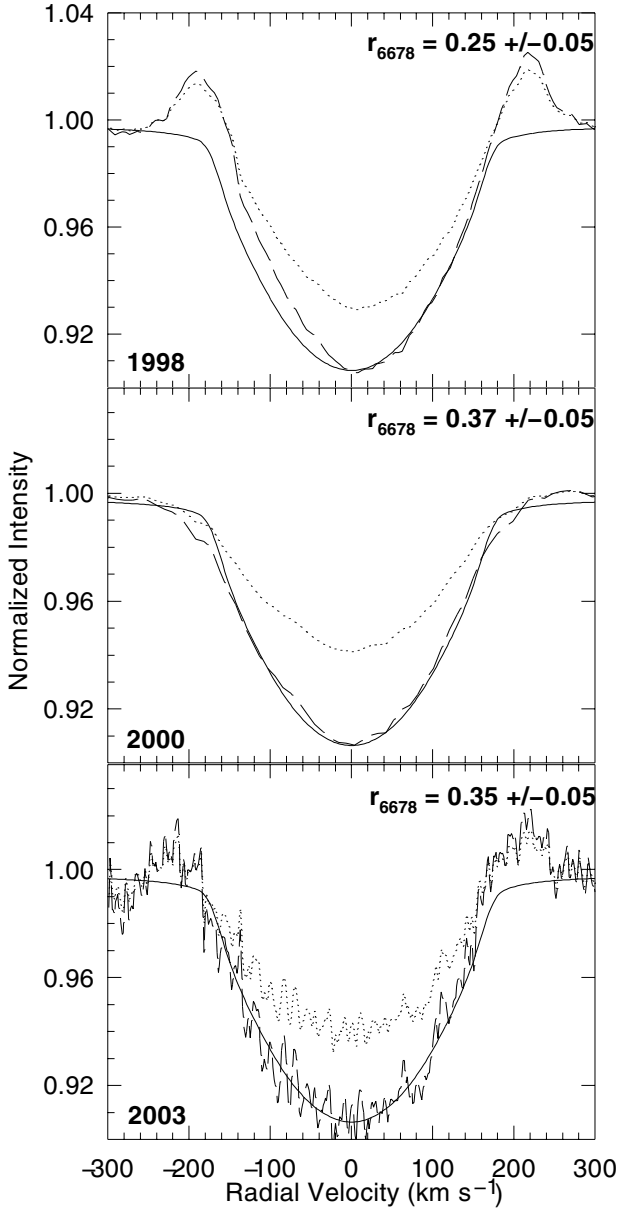

Fig. 20. Time variation of the He I 6678 line profile (dots) compared to the veiling-corrected observed profiles (dashes) and the theoretical photospheric spectrum (solid line).

8.2. Pulsations

The frequencies 2.6 and 3.0 c d^{-1} were found in *lpv* and in spectral parameters of photospheric lines in 2000, as well as in *lpv*, CD, and $V \sin i$ of the He I 6678 line in 1998. Variations with these frequencies found in the CD of the He I 6678 line in 1998 can be an indication of pulsations, and/or of rotation when the star hosts an oblique magnetic dipole field.

The only frequency for which the associated phase velocity could be derived is the 3.0 c d^{-1} frequency, with $\delta\Psi/\pi \sim 3$ (Table 4). The 3.0 c d^{-1} frequency is too high to be related to a rotational modulation effect. Moreover, the first harmonic at ~6 c d^{-1} was detected in the He I 6678 line in 1998 and the C II 4267 line in 2000 with a $\delta\Psi/\pi$ indicative of $|m| \sim 3$. Such a high frequency with $\ell = 3$, $|m| = 3$ was also found in the case of μ Cen (Rivinius et al. 2001). Similarities between these two Be stars is also found elsewhere: they have a moderate $V \sin i$ with $i \sim 30$–40 deg. We thus attribute this frequency to non radial pulsations with $\ell = 3$, $|m| = 3$. According to Rivinius et al. (2003), in the large majority of Be stars, the periodic *lpv* can be explained by non radial pulsations with a mode with $\ell = 2$, $|m| = 2$. Only a few stars in their sample show pulsations with $\ell = 3$, $|m| = 3$. This makes υ Cyg particularly interesting.

Note that a frequency at 1.5 c d^{-1} was also detected in 1998 (see next subsection). The frequency at 3.0 c d^{-1} could thus be considered as twice 1.5 c d^{-1}. However, in 2000, the frequency at 1.5 c d^{-1} is not detected anymore, whereas the frequency at 3.0 c d^{-1} is and has a coherent phase distribution identical to the one observed in 1998. The frequency at 1.5 c d^{-1} is instead associated with rotation (see next subsection).

The case of the 2.6 c d^{-1} is more puzzling, as the greyscale spectra (top panel of Figs. 11, 17 and 18) are typical of non radial pulsations, but the velocity phase could only be easily determined for the He I 4713 line. It seems to be close to $\Delta\Psi/\pi \sim 3$–4. However, modes with $\ell = 4$ are rarely observed in these stars and the mode $\ell = 3$ is more likely. Other measurements of the He I 6678 line in 1998 and blue photospheric lines in 2000 are too uncertain. Moreover, the greyscale spectra for this frequency show a crossed pattern with a bump at velocity 0, indicative more of a zonal mode. It therefore seems that the frequency at 2.6 c d^{-1} corresponds to a zonal mode with $\ell = 3$ (or 4) and $m = 0$. Considering the inclination angle of υ Cyg, the pulsation zones would then be seen on the front side of the star travelling from blue to red and also, with a good contrast, on the rear side of the star travelling from red to blue. This would explain why the phase distributions for this frequency (Fig. 9) is only coherent over small velocity ranges, since we see bumps travelling in both directions. Note that Rivinius et al. (2003) found that the mode $\ell = 3$ (or 4), $m = 0$ is very rare in their sample of Be stars. However, this mode is also very difficult to detect because of the mixed phase distribution. In addition, note that the frequency at 2.6 c d^{-1} may also have a transient character. Indeed, the pattern observed in the greyscale spectra for this frequency could be compared to the one obtained by Rivinius et al. (2003; their Fig. 15) for the transient period of η Cen. However, in υ Cyg, the 2.6 c d^{-1} frequency is mostly observed in the He I 4713 line, which is only marginally influenced by contributions from the inner circumstellar disk.

Since the observations were obtained only on one site at a time, strong aliases were observed in the frequency spectrum, in particular the 1-day alias. It is thus no surprise that a frequency at 1.6 c d^{-1} was also obtained in the TSA (Tables 3 and 5). No velocity phase was found for this frequency, even in parts of those line profiles which show higher signal power, so we can safely discard it from the list of real frequencies.

In the data from 2000, the mean velocity of each line was shifted to zero to be able to study the *RV* variations of all the measured lines. The amplitude of variations was about 12.5 km s^{-1} at the beginning of the observing run. Looking at the *RV* variation of He I lines in time, one can see that the amplitude of variation decreased at HJD 2 451 809-13. The amplitude seemed to be only 5 km s^{-1} at the middle of the run when, for the only time of the observing campaign, the Hides

observations were followed by TBL observations. This could have been due to a beating effect between two closely spaced frequencies, one of them being maybe a temporary period related to the outburst.

As proposed in Sect. 8.1 the lack of clear variation for the He I 6678 line in 2000 (top panel of Fig. 8) could be explained by the outburst which occured during the observations. Another explanation could be damping of the amplitude of the pulsations due to a beating effect. Observations of this line were obtained only at TBL, i.e. after HJD 2 451 809, when the amplitude of the *RV* variations in He I 6678 also decreased. If this phenomenon is related to a beating effect, we can estimate its period to about 8 days, which corresponds to a difference between the 2 frequencies causing the beating of 0.125 c d^{-1}. This value is similar to the minimum detectable frequency for our observations, so we cannot distinguish these 2 frequencies if they exist.

8.3. Rotation

In 1998, the 1.5 c d^{-1} frequency dominated in the *V* and *R* emissions peaks. The strong variation of these emission peaks also produced a variation at the centre of the line with the same frequency. The *RV* data of the He I 6678 line also clearly varied with the 1.5 c d^{-1} frequency. The peak-to-peak amplitude of variations was about 18 km s^{-1}, whereas for the Hα emission peak the amplitude was ~21 km s^{-1}. However, the *RV* maxima and minima were different from one night to the next.

The *V*, *R*, and *V*/*R* observed for the He I 6678 line also displayed strong variations with the frequency at 1.5 c d^{-1} as shown in Fig. 12. *V* and *R* quantities were often varying in opposition of phase (Fig. 7). Several maxima of *V*/*R* were observed during the run, but this maximum value was variable in time. It seemed to reach a maximum value of 1.025 around HJD 2 451 006.6 and then decreased to 1.006 at the end of the observing run.

We conclude that the 1.5 c d^{-1} frequency is probably related to a rotational phenomenon linked to the small outburst revealed by the increase in the quantity $V + R$ at the middle of the 1998 run. If 1.5 c d^{-1} is the rotation frequency itself, then it corresponds to $\frac{\Omega}{\Omega_c}$ around 0.85 (see Table 2), typical of classical Be stars (Chauville et al. 2001; Frémat et al. 2005).

8.4. Model

To test the results presented above, we perform a serie of models. The computer code we use is based on a grid of NLTE stellar models calculated with TLUSTY (Hubeny & Lanz 1995) with steps of 1000 K in temperature, 0.2 dex in log g, and 0.05 in projection angle. We use a solar chemical composition. Perturbations due to non radial pulsations and fast rotation are calculated with a modified version of Bruce/Kylie (Townsend 1997), which provides the corrected stellar parameters at each point on the visible stellar hemisphere. We use a surface grid of ~50 000 points. Integration over the stellar disk is then performed. The final result is a series of time-resolved synthetic spectra of the rotating pulsating star.

The modified version of the code we use is similar to Bruce/Kylie for the pulsations and rotation, but it also integrates the effect of a magnetic dipole field (Neiner et al. 2005). However, no magnetic field is assumed for υ Cyg and the results are thus similar in this case to what Bruce/Kylie would produce.

First we compute 101 spectra per model with either $|f_{\rm puls}|$ = 2.95 c d^{-1} or $|f_{\rm puls}|$ = 2.6 c d^{-1}. From the modeled line profiles, we produce greyscale plots of the variation of the line profiles over the pulsation phase. The wavelength resolution of the synthetic spectra is 0.1 Å, typical of the observations. Models of line profiles and their variations are produced using the parameters determined in Sect. 5. It appears that changes permitted by models B–D (see Table 2) in stellar parameters such as temperature do not modify the models significantly. Therefore we adopt an average temperature $T_{\rm eff}$ = 19 800 K, i.e. a temperature consistent with Case D. Significant changes in i or $f_{\rm rot}$, however, alter the resulting models, and, of course, so do changes in the pulsation frequencies. In particular, how the pulsation frequency compares to the rotation frequency is a major factor. However, small changes in these quantities do not affect the results significantly and, as a first step, we can use approximate parameters for the models. We choose $i = 33°$ and $f_{\rm rot}$ = 1.48 c d^{-1}, because they are close to the parameters determined from our observations (see Sect. 8.3).

Figure 21 shows the results obtained for $|f_{\rm puls}|$ = 2.95 c d^{-1} with $0 \leq \ell \leq 4$ and $-4 \leq m \leq 4$, and Fig. 22 shows the same but for $|f_{\rm puls}|$ = 2.6 c d^{-1}. Temperature and area effects are taken into account (see Townsend 1997), except for the modes with $m = -2$ for $|f_{\rm puls}|$ = 2.95 c d^{-1}, for which only area effects are taken into account because the temperature effects create strong instabilities. The corotation period of a mode is, by definition, positive. Therefore, only the modes for which the corotation period is positive are displayed in the figures, which is why some modes in the figures are computed with a negative $f_{\rm puls}$ and positive m value but look like prograde modes (see Maintz et al. 2003).

Visual comparison of these figures with the corresponding observations (Fig. 17) shows that the pattern with $|f_{\rm puls}|$ = 2.95 c d^{-1} is correctly reproduced by a mode with ℓ=3, m = 3 and $f_{\rm puls}$ negative. We conclude that the pulsation parameters for this mode are ℓ = 3, m = 3 and $f_{\rm puls}$ = −2.95 c d^{-1}. Since the pulsation frequency is an *observed* frequency, a negative $f_{\rm puls}$ is not unphysical but instead the effect of rapid rotation which causes a retrograde ($m > 0$) mode to appear prograde (i.e. with bumps travelling from blue to red) to the observer (see also Rivinius et al. 2001).

The crossed pattern observed for $|f_{\rm puls}|$ = 2.6 c d^{-1} seems to be best reproduced by a mode with ℓ = 3 or 4, m = 0, and $f_{\rm puls}$ positive in the centre and in the red wing of the line, but there is a phase lag in the blue wing. This difference may be due to another undetected pulsation frequency not included in the model or, more probably, to the observed small outburst and ejection of material.

We then compute 201 spectra, sampling a 73.84-h period with one spectrum every ~22 min and modeling both pulsation frequencies at the same time. This number of spectra and period of time were chosen so that each of the two frequencies

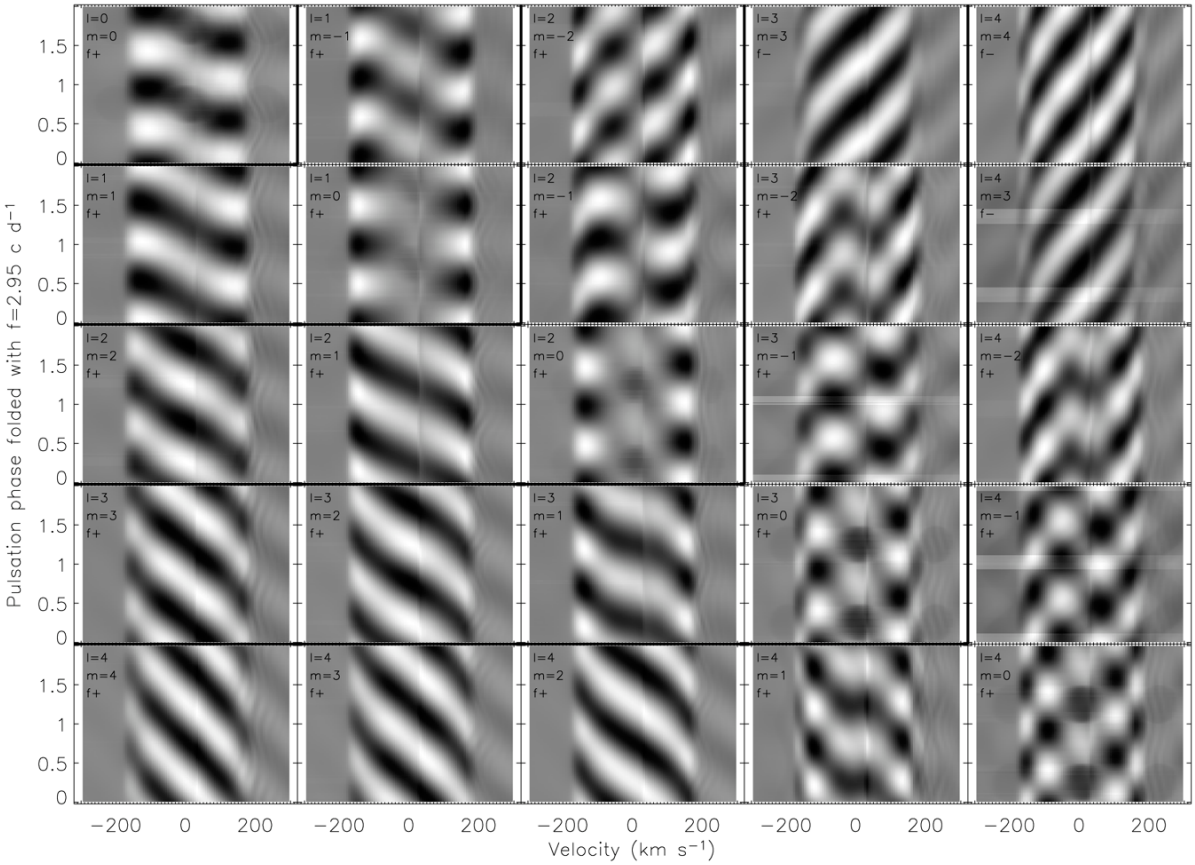

Fig. 21. Catalog of pulsation models of the He I 4713 line, using $T_{\rm eff}$ = 19 800 K, i = 33°, $f_{\rm rot}$ = 1.48 c d^{-1} and $f_{\rm puls}$ = 2.95 c d^{-1} for $0 \le \ell \le 4$ and $-4 \le m \le 4$. For each model the legend indicates the values of ℓ and m and whether the $f_{\rm puls}$ was assumed positive or negative. Only models for which the corotation frequency is positive are displayed.

(−2.95 and 2.6 c d^{-1}) are well sampled in phase and the time is longer than the beating period (2.5 d). From the modeled line profiles, we again produce greyscale plots of the variation of the line profiles over the pulsation phase. The spectra are averaged by bins of 0.05 in phase to mimic the time sampling of the observations. The wavelength resolution of the synthetic spectra is 0.1 Å, typical of the observations.

Combining the two modes show that the combination of the mode at $\ell = 3$, $m = 3$ for $f_{\rm puls} = -2.95$ c d^{-1} with the zonal mode at $f_{\rm puls} = 2.6$ c d^{-1} reproduces the patterns observed in Fig. 17. Using the mode $\ell = 3$, $m = 0$ or the mode $\ell = 4$, $m = 0$ for $f_{\rm puls} = 2.6$ c d^{-1} gives very similar results. Therefore, we cannot distinguish from the models which of the two zonal modes is the one in υ Cyg. The results found from the models are thus in agreement with the pulsation parameters determined in Sect. 6: $\ell = 3$, $m = 3$ and $\ell = 3$ or 4, $m = 0$.

Figure 23 shows the final results when assuming the two modes of pulsations simultaneously. The stellar parameters used are those of Cases C and D (see Sect. 5). The pulsation frequencies used are those determined in Sect. 6, i.e. $f_{\rm puls} = -2.95$ c d^{-1} and $f_{\rm puls} = 2.6$ c d^{-1}. The first pulsation mode has the parameters $\ell = 3$, $m = 3$ and the second mode has the same ℓ but $m = 0$. Both modes have the same amplitude. Figure 23 shows that the mode with $\ell = 3$, $m = 3$ appears smeared out in the centre of the line when the rotation rate is higher (Case D) as observed in Fig. 17. However, the mode with $\ell = 3$, $m = 0$ also appears less sharp in the centre of the line, whereas the observations show a clear pattern. An explanation could be found in the amplitude of the modes, e.g. if the zonal mode has a higher amplitude than the other mode. We conclude that the models do not allow us to determine the stellar parameters more accurately than in Sect. 5.

8.5. Binarity

υ Cyg is given as a possible spectroscopic binary in the Bright Star Catalogue, and it has an ADS number. However, Abt & Cardona (1984) found that the B and C components do not form a multiple system with υ Cyg, but are instead foreground stars. Abt & Levy (1978) also found that the RV of υ Cyg is constant. Moreover, no sign of a companion has been detected with Speckle analysis (Hartkopf & McAlister 1984).

It seems from our mean profiles, however, that the centre of the Hα (Fig. 4) and He I 6678 (Fig. 3) lines is variable with time. The RV deduced from the Hα profiles are 10.6 km s^{-1} in 1998, −4 km s^{-1} in 2000 and −7.5 km s^{-1} in 2003. From data taken from Buil (2004) we also measure RV = 0 km s^{-1} in 1999 and −17 km s^{-1} in 2002. This variation could be due to a companion. A fit of the RV data (Fig. 24) gives an estimate of 11.4 years for the binarity period. This is consistent with the lower limit for a binarity period of 10 years given in the Hipparcos catalogue (Perryman 1997).

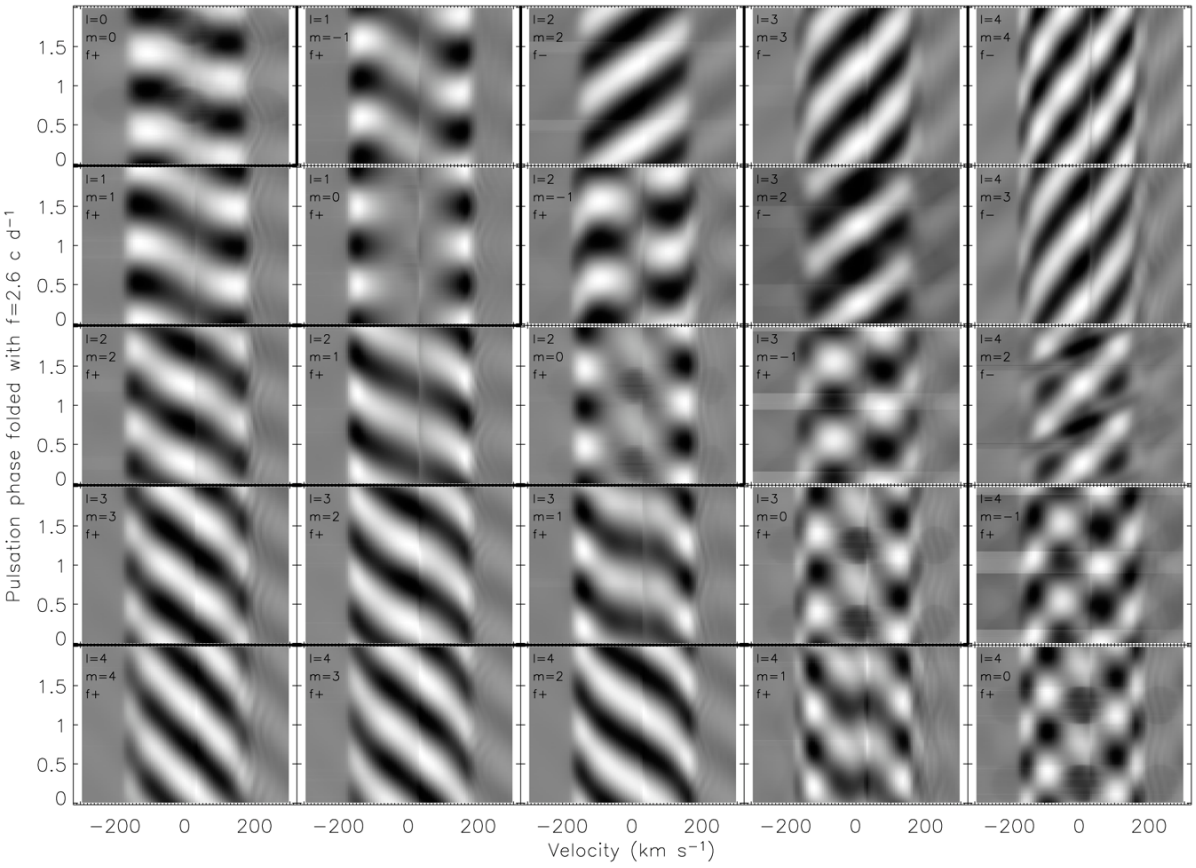

Fig. 22. Same as Fig. 21 but with $f_{\rm puls}$ = 2.6 c d^{-1}.

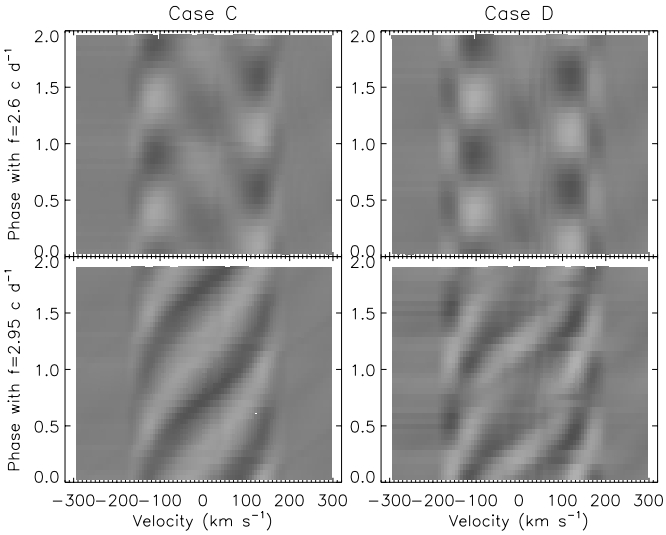

Fig. 23. Pulsation model with two modes at ℓ = 3, m = 0, $f_{\rm puls}$ = 2.6 c d^{-1} and ℓ = 3, m = 3, $f_{\rm puls}$ = −2.95 c d^{-1} for the stellar parameters of Cases C and D. *Top panel*: folded in phase with f = 2.6 c d^{-1}. *Bottom panel*: folded in phase with f = 2.95 c d^{-1}.

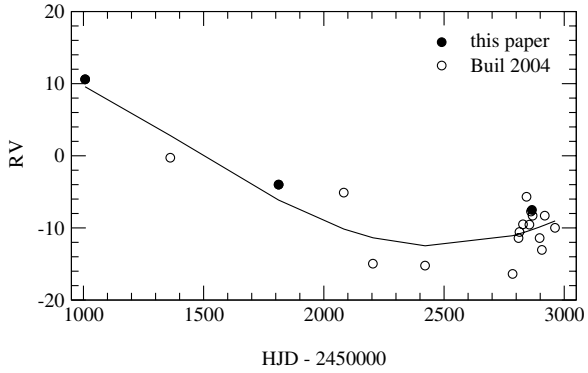

Fig. 24. Radial velocity variations (in km s^{-1}) of the Hα line on a long timescale, indicative of a possible binarity.

9. Conclusion

υ Cyg is a very active Be star that undergoes numerous outbursts. Weaker outbursts occur every ∼1400 days between stronger ones. During each of our observing runs in 1998, 2000, and 2003, we observed an outburst. In particular, the one in 2000 was of similar intensity to the one in 1992.

Multiperiodic non-radial pulsations are detected in this star with frequencies at 2.95 and 2.6 c d^{-1}. The observed patterns are well reproduced by models of a retrograde g-mode with ℓ = 3, m = 3 and a zonal g-mode with ℓ = 3 (or 4), m = 0, respectively. Another frequency at 1.5 c d^{-1} is associated with rotational phenomena. This value is coherent with the rotation frequency deduced from the stellar parameters.

Moreover, the peak-to-peak amplitude of variations seems to vary in time, maybe due to a beating effect between close

frequencies. The resolution in time of our data, however, does not allow us to separate such close frequencies.

Finally, a longer timescale variation may be present, with a period around 11.4 years, which could be associated with a binary companion.

Acknowledgements. C.N. wishes to thank I. Hubeny & T. Lanz and R. Townsend for making TLUSTY and BRUCE (respectively) publicly available. We thank V. Desnoux for her help with the "Buil data" and the referee, S. Štefl, for constructive comments. This research has made use of the Simbad database maintained at CDS, Strasbourg, France.

References

Abt, H. A., & Levy, S. G. 1978, ApJS, 36, 241
Abt, H. A., & Cardona, O. 1984, ApJ, 285, 190
Ballereau, D., Alvarez, M., Chauville, J., & Michel, R. 1987, Rev. Mex. Astron. Astrofis., 15, 29
Ballereau, D., Chauville, J., & Zorec, J. 1995, A&AS, 111, 423
Buil, C. 2004, Be stars Atlas on the web, http://www.astrosurf.com/buil/us/bestar.htm
Campbell, W. W. 1895, ApJ, 2, 177
Chauville, J., Zorec, J., Ballereau, D., & Morrell, N. 2001, A&A, 378, 861
Collins, G. W., Truax, R. J., & Cranmer, S. R. 1991, ApJS, 77, 541
Donati, J.-F., Semel, M., Carter, B., et al. 1997, MNRAS, 291, 658
Fleming, M. 1891, AN, 128, 403
Floquet, M., Neiner, C., Hubert, A. M., et al. 2000, in The Be Phenomenon in Early-Type Stars, IAU Coll. 175, ed. M. A. Smith, H. Henrichs, & J. Fabregat, ASP Conf., 214, 260
Floquet, M., Neiner, C., Janot-Pacheco, E., Hubert, A. M., et al. 2002, A&A, 394, 137
Frémat, Y., Zorec, J., Hubert, A.-M., & Floquet, M. 2005, A&A, in press [arXiv:astro-ph/0503381]
Gray, D. F. 1976, The observation and analysis of stellar photospheres (Wiley-Interscience)
Hanuschik, R. W., Hummel, W., Dietle, O., & Thimm, G. 1996, A&AS, 116, 309
Hartkopf, W. I., & McAlister, H. A. 1984, PASP, 96, 105
Hubeny, I., & Lanz, T. 1995, ApJ, 439, 875
Hubert, A.-M., & Floquet, M. 1998, A&A, 335, 565
Hubert-Delplace, A.-M., & Hubert, H. 1979, An Atlas of Be Stars, Paris-Meudon Observatory
Hubert-Delplace, A.-M., Hubert, H., Ballereau, D., & Chambon, M. T. 1982, IAU Symp., 98, 195
Hubert, A. M., Floquet, M., & Zorec, J. 2000, in The Be Phenomenon in Early-Type Stars, IAU Coll. 175, ed. M. A. Smith, H. Henrichs, & J. Fabregat, ASP Conf., 214, 348
Hummel, W., & Dachs, J. 1992, A&A, 262, L17
Hummel, W., & Vrancken, M. 1995, A&A, 302, 751
Jankov, S., Janot-Pacheco, E., & Leister, N. 2000, ApJ, 540, 535
Kurucz, R. 1994, CD-ROM No. 19, Cambridge, Smithsonian Astrophysical Observatory
Maintz, M., Rivinius, Th., Štefl, S., et al. 2003, A&A, 411, 181
Mennickent, R. E., Pietrzyǹski, G., Gieren, W., & Szewczyk, O. 2002, A&A, 393, 887
Neiner, C., Hubert, A.-M., Floquet, M., et al. 2002, A&A, 388, 899
Neiner, C., Solanki, S., & Frémat, Y. 2005, A&A, in preparation
Oudmaijer, R. D., & Drew, J. E. 1997, A&A, 318, 198
Percy, J. R., Harlow, C. D., & Wu, A. P. S. 2003, A&AS, 202, 3901
Peters, J. 1979, ApJS, 39, 175
Perryman, M. A. C. 1997, The Hipparcos and Tycho catalogues, ESA-SP 1200, published in Noordwijk, Netherlands
Porter, J. M., & Rivinius, Th. 2003, PASP, 115, 1153
Rivinius, Th., Baade, D., & Štefl, S. 2003, A&A, 411, 229
Rivinius, Th., Baade, D., Štefl, S., et al. 1998, A&A, 336, 177
Rivinius, Th., Baade, D., Štefl, S., et al. 2001, A&A, 369, 1058
Schaller, G., Schaerer, D., Meynet, G., & Maeder, A. 1992, A&AS, 96, 269
Slettebak, A., & Reynolds, R. C. 1978, ApJS, 38, 205
Smith, M. A., Hubeny, I., & Lanz, T. 1994, IAU Symp., ed. L. A. Balona, H. F. Henrichs, & J.-M. Le Contel (Kluwer Academic Publishers), 162, 273
Telting, J. H., & Schrijvers, C. 1997, A&A, 317, 723
Townsend, R. H. D. 1997, MNRAS, 284, 839
Townsend, R. H. D., Owocki, S. P., & Howarth, I. D. 2004, MNRAS, 350, 189
Tubbesing, S., Rivinius, Th., & Wolf, B. 2000, in The Be phenomenon in early-type stars, IAU Coll. 175, ed. M. A. Smith, H. F. Henrichs, & J. Fabregat, ASP Conf. Ser., 214, 232